Application of a band-crossing model for resonances in $^{16}O+^{16}O$ scattering

Yosio Kondō* and D. A. Bromley
A. W. Wright Nuclear Structure Laboratory, Yale University, New Haven, Connecticut 06520

Yasuhisa Abe
Centre de Recherches Nucléaires, 67037 Strasbourg, France and Research Institute for Fundamental Physics, Kyoto University, Kyoto 606, Japan

(Received 28 February 1980)

A band-crossing model that has been proposed as a possible mechanism for resonances in heavy ion reactions is applied to energy dependent structure in the $^{16}O+^{16}O$ system. The recently observed intermediate-width structure in the 6.13 MeV gamma-radiation yield can be well understood in terms of the band-crossing model, assuming the crossing of the elastic potential resonance band and an aligned rotational band in which the intrinsic spin ($3\hbar$) and the relative angular momenta are coupled to their maximum value. Numerical calculations based on this model reproduce all of the observed energy dependent structure of the cross section in the $^{16}O+^{16}O$ interaction, i.e., the gamma-radiation yield from the 3_1^- state of ^{16}O, as well as the total fusion and elastic scattering data. Each oscillation in the fusion excitation function is interpreted as reflecting a shape resonance of each new grazing partial wave in the entrance channel as it becomes active with increasing energy. The observed anticorrelation of the total fusion and the 90° excitation function of elastic scattering data is reproduced naturally by the model. It is concluded that these data support the existence of nuclear molecular resonances in the $^{16}O+^{16}O$ system.

[NUCLEAR REACTIONS $^{16}O+^{16}O$ scattering, $10 \leq E_{c.m.} \leq 41$ MeV; calculated elastic scattering excitation functions, fusion cross sections, and 3_1^- inelastic cross sections. Resonance mechanism for heavy ion reactions.]

I. INTRODUCTION

Since the observation of three resonances[1] correlated in different cross sections in the sub-Coulomb $^{12}C+^{12}C$ reaction, it has been recognized[2] that resonant phenomena in heavy ion reactions provide an interesting problem involving both the interaction between composite nuclei and the nuclear structure of the composite system in highly excited states. One of the long standing questions in the study of these quasimolecular phenomena was the apparent absence[1] of resonant states in the Coulomb barrier region in the $^{16}O+^{16}O$ system when they appear in others, particularly in $^{12}C+^{12}C$.

The recent total fusion cross section measurements of Fernandez *et al.*[3] and measurements of Kolata *et al.*[4] on gamma radiation deexciting the 6.13 MeV 3_1^- state of ^{16}O, in addition to the much older elastic scattering data of Maher *et al.*,[5] reveal the existence of pronounced energy dependent structure in the corresponding $^{16}O+^{16}O$ system excitiation functions at energies well above the Coulomb barrier. As we shall demonstrate in the present paper, our examination of these data suggests that nuclear molecular resonances are responsible for the observed structure in the $^{16}O+^{16}O$ system. The absence of resonant states in the Coulomb barrier region in the $^{16}O+^{16}O$ system reflects not the absence of nuclear molecular phenomena but rather their being masked by a great many nonresonant amplitudes.

Scheid *et al.*[6] suggested that the intermediate-width structure in the elastic scattering excitation functions reflected a double resonance mechanism involving both a virtual resonance in the entrance channel and resonant excitation of one—or both—of the ^{16}O nuclei. More recently, Phillips *et al.*[7] have shown that the structure in the inelastic scattering excitation function in the $^{16}O+^{16}O$ data involving the lowest 3_1^- excitation can be reproduced using Hahne's[8] modified Austern-Blair[9] formalism; such a model includes no explicit resonance mechanisms and the structure reflects overlap of angular momentum windows in the entrance and the exit channels. Friedman *et al.*[10] have, however, suggested a reinterpretation of these angular momentum window effects as reflecting the presence of ion-ion barrier top resonances and have shown that similar results can be obtained based on the Born approximation. However, these approaches, except for that of Scheid *et al.*, are approximations to the coupled-channel formalism and they have an inherent difficulty. Since the excited state of the ^{16}O nucleus has a strongly collective nature, the Born approximation would not be expected to provide a good approximation for the description of inelastic scattering to this state. This is also true for Hahne's approximation, which is essentially based on the same approximation as does

the distorted wave Born approximation (DWBA). There is an example[11] in which the cross section for collective 2_1^+ inelastic scattering—calculated with the DWBA—is compared with that predicted in a coupled-channel calculation for the $^{12}C+^{12}C$ system. At an energy where the angle integrated cross section of the 2_1^+ inelastic scattering shows a peak, $E_{c.m.}=25$ MeV, the former gives a cross section four to five times larger than the latter and the calculated angular distributions are quite different in the two approaches. This strongly suggests the importance of higher order effects. In this respect, it is interesting to perform numerical calculations based on a coupled-channel formalism, in which these higher order effects are taken into account.

It is our purpose in this paper to attempt to clarify the underlying mechanism of the structure in the energy dependence of $^{16}O+^{16}O$ cross sections by applying a band-crossing model[12-20] (BCM) in a consistent fashion to all the available data on the $^{16}O+^{16}O$ interaction. The BCM has been proposed as a possible mechanism for resonances in heavy ion reactions by Matsuse and two of the present authors (Y.K. and Y.A.) and has been demonstrated to reproduce characteristic features of elastic and inelastic scattering data for both the $^{12}C+^{12}C$ and $^{12}C+^{16}O$ systems in which prominent resonant phenomena have been observed. As we shall demonstrate herein, a simple coupled-channel calculation, based on the BCM, in which only elastic and aligned 3_1^- inelastic channels are included provides a quite reasonable reproduction of the inelastic scattering, fusion cross sections, and elastic excitation functions of the $^{16}O+^{16}O$ system at the same time.

It should be noted that although some of the data have been reproduced by previous models,[5,7,10] this is the first consistent reproduction of all available data on the energy dependence of the $^{16}O+^{16}O$ system. The structure observed in the 3_1^- gamma-radiation yield[4] can be understood as a consequence of strong mixing of wave functions in the elastic and the aligned inelastic molecular bands, in the energy region where the two bands approach and cross. The structure in the fusion excitation function[3] and the structure in the elastic scattering excitation functions[5] can be understood as entrance channel phenomena, which reflect shape resonances for individual grazing partial waves in the entrance channel. Our results also suggest that the deep minima in the elastic 90° excitation function result from destructive interference between resonant and background amplitudes and explains the anticorrelation[21] between these and the fusion data in natural fashion.

In Sec. II of this paper, a schematic illustration of the BCM is given. The formalism of the BCM using a coupled-channel approach is introduced in Sec. III. Results and discussion are presented in Sec. IV. A summary and concluding discussion comprise Sec. V.

II. THE BAND-CROSSING MODEL

In this section we review briefly the salient features of the band-crossing model as it applies to the $^{16}O+^{16}O$ system. In this model we assume the existence of a series of bound or quasibound states in the elastic channel. These are readily obtained with any reasonable choice of the interaction potential between the two interacting nuclei. Existence of an elastic molecular band in the $^{16}O+^{16}O$ system was predicted by Scheid *et al.*,[6] and by Arima *et al.*,[22] on the basis of the Gobbi potential,[23] evolved empirically to fit elastic scattering data, and also from microscopic studies[24-26] of interactions between composite particles. In this elastic molecular band the two ^{16}O clusters are assumed to remain in their respective ground state. The energies of states in the band are simply approximated by a rotational expression,

$$E_J^{(0)}=(\hbar^2/2\mathcal{I})J(J+1)+E_0^{(0)}\,. \tag{1}$$

In our case we have adjusted the band head energy $E_0^{(0)}$ to yield an 18^+ resonance at an energy $E_{c.m.}=26.5$ MeV where the $^{16}O(^{16}O,^{12}C)^{20}Ne$ reaction[27] provides strong evidence for it. $\mathcal{I}$ and J are the moment of inertia and the total angular momentum of the system, respectively.

Invoking an excitation of one of the ^{16}O ions to its 3_1^- state ($E_x=6.13$ MeV) during the interaction—as originally suggested in the Nogami-Imanishi model[28,29]—yields a set of four additional excited molecular bands. In zeroth order approximation, the energies of states in these bands are given by Eq. (2):

$$E_J^{(I_c)}=(\hbar^2/2\mathcal{I})L_c(L_c+1)+E_0^{(0)}+\epsilon_c\,, \tag{2}$$

where I_c, L_c, and ϵ_c are the channel spin, the relative angular momentum, and the internal excitation energy (6.13 MeV in this case), respectively. The energies of these states are shifted from the elastic ones by the excitation energy ϵ_c. Although they have the same level spacing as the elastic band, their relative angular momenta L_c are shifted from the total angular momenta J because of the coupling with the channel spin I_c. As a consequence of the angular momentum coupling and the parity selection rule, bands having total angular momenta $J=L_c-3$, L_c-1, L_c+1, L_c+3 are produced. These inelastic molecular bands are illustrated in Fig. 1 together with the elastic one. The fact that the four inelastic bands have different

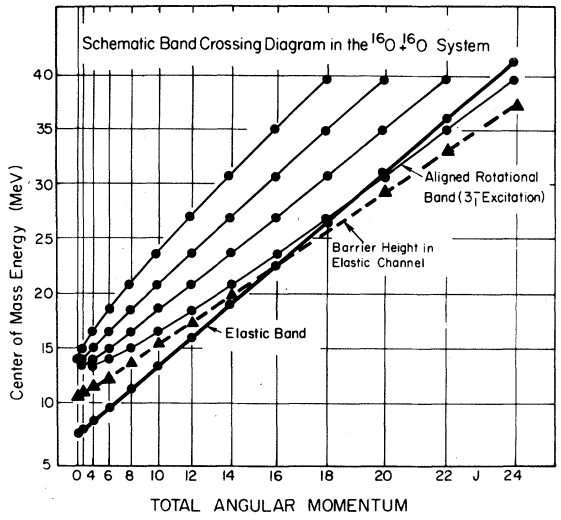

FIG. 1. Illustration of the band-crossing model for the $^{16}O+^{16}O$ system. The elastic rotational band and inelastic 3_1^- bands are included. The band head energy of the elastic band is adjusted to reproduce an 18^+ resonance at an energy $E_{c.m.}=26.5$ MeV, as experimental data (Ref. 27) suggested. The dotted line shows the height of the potential barrier in the elastic channel.

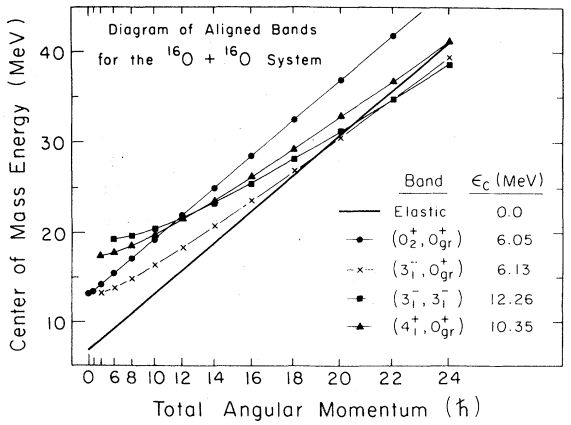

FIG. 2. Band crossing diagram for aligned bands in the $^{16}O+^{16}O$ system. Aligned rotational bands corresponding to excitations of the 0_2^+ state (6.05 MeV), the 3_1^- state (6.13 MeV), the 4_1^+ state (10.35 MeV), and mutual excitation of the 3_1^- state are plotted together with the elastic one. These aligned bands, except for the 0_2^+ excitation, cross the elastic one at relatively low total angular momenta.

slopes in this figure reflects the shifts of the relative angular momenta L_c in Eq. (2) rather than a change in the moment of inertia. However, these states in the inelastic molecular bands are not always observed as resonances. Whether they are observed as prominent resonances or not depends crucially upon coupling between relevant channels. If a state has significant partial widths for both the entrance (Γ_{in}) and exit (Γ_{out}) channels, the state will be observed as a resonance state in the relevant processes, as expected from a simple Breit-Wigner expression:

$$\sigma(E)=\frac{2\pi}{k^2}(2J+1)\frac{\Gamma_{in}\Gamma_{out}}{(E-E_R)^2+\Gamma_{tot}{}^2/4}, \qquad (3)$$

where E_R, Γ_{tot}, Γ_{in}, and Γ_{out} are the resonance energy, total width, and partial widths for the entrance and exit channels, respectively. In this equation the additional factor of 2 reflects the fact that we are dealing with an identical particle system. Obviously the magnitude of the partial widths participating in a given resonance depends upon the strength of the coupling interaction. At the same time, however, it also depends upon the energy separation (as in Fig. 1) of the pertinent molecular band states, and thus upon the extent to which these states mix.

Crucial to the BCM is the fact that the elastic and one of the inelastic bands cross in the region of interest; this lowest of the inelastic bands is always the aligned one in which the orbital angular momentum L_c and the channel spin I_c are additive, i.e., $J=L_c+I_c$. The energy and total angular momentum at, or nearest to, the crossing point can be estimated by equating Eqs. (1) and (2). The wave functions of states in the two bands would be expected to mix strongly in the crossing region, thus providing a mechanism whereby the unexcited ions in the entrance channel can couple readily to an exit channel in which one of the ions is left in its 3_1^- state, i.e., to an inelastic channel. Thus the BCM predicts enhanced 3_1^- inelastic cross sections at the band crossing region. This is the excitation mechanism that the BCM predict.

In Fig. 2, some of aligned molecular bands in the $^{16}O+^{16}O$ system which cross the elastic band at relatively low total angular momentum are plotted together with the elastic one. The excitations included are the 0_2^+ state (6.05 MeV), the 3_1^- state (6.13 MeV), the 4_1^+ state (10.35 MeV), and mutual excitation involving the 3_1^- state. The 0_2^+ and 4_1^+ states have well-developed α-cluster structure.[30] The 3_1^- state has a strongly collective nature with strong inelastic matrix element connecting it to the ground state. As is clear from this figure, different excitations lead to different crossing points depending upon both internal excitation energies and intrinsic angular momenta; in simplest approximation the inelastic band corresponding to the 0_2^+ state never crosses the elastic one. In other words, the BCM predicts a systematic change in the dominant inelastic excitation component of the interaction as the incident energy, hence angular momentum, increases. This prediction of the BCM was studied in detail in the

$^{12}C+^{12}C$ system,[15] and has been confirmed in recent experiments.[31] This prediction is also useful as a guide in selecting the model space for numerical calculations at any given energy.

As shown in Fig. 2, the lowest energy crossings occur between the elastic band and aligned bands corresponding to the single and mutual excitation of the 3_1^- state at center of mass energies near 30 MeV and with total angular momenta in the 18 $\sim 22\hbar$ range. It bears emphasis that the observed structure in the 3_1^- gamma-radiation yield data corresponds to this energy region.

Another important question that can be addressed within the framework of the BCM concerns the widths of the resonances. These can be estimated roughly by comparing the resonance energies with the height of the relevant potential barrier, although they are also influenced by flux flow to other channels, i.e., by the imaginary part of the optical potential.

Following our discussion of Eq. (1) above, the barrier heights ($B_J^{(0)}$) of the potential in the entrance channel are approximately given as follows [Eq. (4)] and as illustrated in Fig. 1:

$$B_J^{(0)}=\frac{\hbar^2}{2\mu R_b^2}J(J+1)+V_{\mathrm{Coul}}(R_b)+C_N\,, \tag{4}$$

where the Coulomb potential $V_{\mathrm{Coul}}(r)$ is

$$V_{\mathrm{Coul}}(r)=\begin{cases}\dfrac{Z_1Z_2e^2}{r} & \text{for } r\geq R\\[2ex] \dfrac{Z_1Z_2e^2}{2R}\left[3-\left(\dfrac{r}{R}\right)^2\right] & \text{for } r<R\,.\end{cases} \tag{5}$$

μ and R_b are the reduced mass of the system and the radius at which the barrier has its maximum, respectively. C_N presents the contribution from the nuclear potential at this distance R_b. If the energies of the resonances in the band crossing region are well below the barriers in both channels, penetrability arguments suggest that the resonance widths would be expected to be very narrow and as expected from the Breit-Wigner expression, Eq. (3), the corresponding inelastic yields would be very small. Under such circumstances, it may be difficult to find the resonances experimentally. On the other hand, if the resonances are located at energies well above the barrier in both channels, resonances in adjacent partial waves overlap, and it again may be difficult to recognize resonances in the experimental integrated cross section. In this respect, study of collisions of identical spinless particles has an advantage, since only even values of the total angular momentum J can contribute to the reaction and the energy spacing between adjacent partial wave effects is correspondingly increased. In our case, as shown in Fig. 1, the anticipated resonances—in the band crossing region—are located at energies near the top of the corresponding barrier and would therefore be expected to have an intermediate width that should make them observable in experimental data.

III. FORMULATION OF THE BCM

In order to examine the relevance of the BCM to the above mentioned data, we have carried through a coupled-channel calculation for the $^{16}O+^{16}O$ system, including the elastic and aligned 3_1^- inelastic channels as the BCM would suggest. In this section we briefly summarize the formalism used.

A. Coupled-channel equation

The total Hamiltonian of the $^{16}O+^{16}O$ system can be written as follows:

$$H=h_1(\theta_1)+h_2(\theta_2)+T(r)+U(r,\theta_1,\theta_2)\,, \tag{6}$$

where $h_i(\theta_i)$ is the internal Hamiltonian with internal variable θ_i of the ^{16}O nuclei. $T(r)$ and $U(r,\theta_1,\theta_2)$ are the kinetic operator and the interaction potential for the relative motion between two oxygen nuclei, respectively. The coordinate r measures the separation of the two nuclear centers. The internal wave function $\chi_{I_iM_i}(\theta_i)$ for ^{16}O is an eigenfunction of the internal Hamiltonian $h_i(\theta_i)$,

$$h_i(\theta_i)\chi_{I_iM_i}(\theta_i)=\epsilon_{I_i}\chi_{I_iM_i}(\theta_i)\,, \tag{7}$$

where I_i and M_i are the internal spin and its z component, respectively. The eigenvalue ϵ_{I_i} is set equal to the experimental ones, i.e., $\epsilon_{I_i}=0.0$ and 6.13 MeV for $I_i=0$ and 3, respectively. We assume a phonon model for the internal wave function.

$$\chi_{I_iM_i}=\begin{cases}|0\rangle & \text{for the ground state with } I_i=0\\ b^\dagger_{3M_i}|0\rangle & \text{for the excited state with } I_i=3\,,\end{cases} \tag{8}$$

where $b^\dagger_{IM}$ is a standard phonon creation operator.

The total wave function ψ_{JM_J} of the $^{16}O+^{16}O$ system—with a total angular momentum J and its z component M_J—can be expanded in terms of channel wave functions, as follows:

$$\psi_{JM_J}(r,\theta_1,\theta_2)=\sum_c\frac{1}{r}u_c^J(r)\mathcal{Y}_c^{JM_J}(\hat{r},\theta_1,\theta_2)\,, \tag{9}$$

where

$$\begin{aligned}\mathcal{Y}_c^{JM_J}(\hat{r},\theta_1,\theta_2)=&[2(1+\delta_{I_1I_2})]^{-1/2}S_{12}\\ &\times\sum_{\substack{M_1M_2\\M_IM_L}}(I_1I_2M_1M_2|IM_I)(ILM_IM_L|JM_J)\\ &\times\chi_{I_1M_1}(\theta_1)\chi_{I_2M_2}(\theta_2)Y_{LM_L}(\hat{r})\,,\end{aligned} \tag{10}$$

and $u_c^J(r)$ and $Y_{LM_L}(\hat{r})$ are the radial part of the relative wave function and a standard spherical harmonic, respectively. The operator S_{12} symmetrizes the channel wave function with respect to the exchange of particles 1 and 2. The symbol c is the channel index representing explicit quantum numbers, i.e.,

$$c=[(I_1^c, I_2^c)I_c, L_c]=[(I_1, I_2)I, L]\,. \tag{11}$$

Multiplying $\mathcal{Y}_c^{JM}{}_J^*(\hat{r}, \theta_1, \theta_2)$ through the Schrödinger equation $(H-E)\psi_{JM_J}=0$ and integrating over $\hat{r}$, θ_1 and θ_2, we obtain a set of coupled-channel equations,

$$\sum_{c'} \{[\mathfrak{L}_c(r)-E_c]\delta_{cc'}+V_{cc'}(r)\}u_{c'}^J(r)=0\,, \tag{12}$$

where

$$\mathfrak{L}_c(r)=\frac{-\hbar^2}{2\mu}\left[\frac{d^2}{dr^2}-\frac{L_c(L_c+1)}{r^2}\right]+U_{\rm opt}(r)\,. \tag{13}$$

Here E_c is the energy of relative motion in the channel c, i.e., $E_c=E-\epsilon_{I_1^c}-\epsilon_{I_2^c}$. The total energy of the system E is measured in the incident $^{16}O+^{16}O$ channel. $U_{\rm opt}(r)$ is the usual optical potential. The coupling potential $V_{cc'}(r)$ is defined as follows for $c\neq c'$:

$$V_{cc'}(r)=\langle \mathcal{Y}_c^{JM_J}\,|U(r, \theta_1, \theta_2)|\mathcal{Y}_{c'}^{JM_J}\rangle\,. \tag{14}$$

To solve the coupled-channel equation (12) under the proper boundary condition, we have adopted an extended Mito-Kamimura[32] method based on Kohn and Hulthén's variational principle.[33] This method was discussed elsewhere[18] and we shall not repeat its details here.

B. Interaction potential

The real part of the optical potential $U_{\rm opt}(r)$ is a sum of Coulomb [Eq. (5)] and nuclear terms:

$$\mathrm{Re}U_{\rm opt}(r)=V_{\rm Coul}(r)+U_{\rm nucl}(r)\,. \tag{15}$$

For the nuclear part, we have chosen to use a two range Woods-Saxon shape as follows:

$$U_{\rm nucl}(r)=V_{\rm core}f_{\rm WS}(R_{\rm core}, a_{\rm core}, r) -[V_0+V_JL(L+1)]f_{\rm WS}(R, a, r)\,, \tag{16}$$

where

$$f_{\rm WS}(R, a, r)=\left[1+\exp\left(\frac{r-R}{a}\right)\right]^{-1}\,. \tag{17}$$

The short range repulsive component has been included to reflect the effects of Pauli exclusion. The longer range attractive component is chosen to have an angular momentum dependence, in which partial waves with higher relative angular momenta feel a stronger attractive nuclear force. Both of these features emerge from microscopic studies[26,34] of the interaction between composite particles. The parameters of the interaction potential used in the present calculation are listed in Table I. The repulsive core is represented by $V_{\rm core}=100$ MeV, $a_{\rm core}=0.3$ fm, and $R_{\rm core}=3.5$ fm. This core radius was estimated from the range of the outermost node of the microscopic relative wave function[26] that is considered to be the origin of the structural core[35,36] of the interaction between composite nuclei. The attractive well has parameters $V=16.0+0.014L(L+1)$ MeV, $R=6.55$ fm, and $a=0.5$ fm. The real part of these potentials, including the centrifugal term, is plotted in Fig. 3 for relative angular momenta $L=0\sim30$. As is shown in this figure, the real potential has a minimum for $L<24$. Barrier heights, energies, and widths of potential resonances in the elastic and aligned 3_1^- inelastic channels are given in Table II. These values were calculated for the potential of Fig. 3, i.e., with no coupling and with no imaginary part. The resonances in each channel form a band and can be well described as rotational sets—Eqs. (1) and (2)—as discussed in the previous section. Crossing of the two bands takes place at a spin value between $J=18$ and 20. An elastic resonance with $J=18$ appears at $E_{\rm c.m.}=26.6$ MeV which satisfies the requirement of the $^{16}O(^{16}O, {}^{12}C)^{20}Ne$ data[27] mentioned in Sec. II. As seen from Table II, single particle widths $\Gamma_{\rm sp}$ of the resonances are closely related to the energy difference between the resonance and the barrier top.

In introducing a coupling potential, we follow the procedure of Ref. 37. The effect of the internal motion of the nuclei is introduced via the range

TABLE I. Adopted parameters for our interaction potential. The part labeled "core" represents a short range repulsive core reflecting effects of the Pauli principle. The depth of the real attractive potential is given by $V_0+V_JL(L+1)$. Both the core and attractive parts are assumed to have Woods-Saxon shape. The imaginary part of the interaction potential has an explicit J dependence and is defined by Eqs. (20) and (21). γ measures the strength of the coupling to the 3_1^- excitation.

Core part			Attractive part			
$V_{\rm core}$ (MeV)	$R_{\rm core}$ (fm)	$a_{\rm core}$ (fm)	V_0 (MeV)	V_J (MeV)	R (fm)	a (fm)
100.0	3.50	0.30	16.0	0.014	6.55	0.50

Imaginary part				Coupling
W (MeV)	$\bar{Q}$ (MeV)	$\bar{R}$ (fm)	ΔJ (N.D.)	γ (N.D.)
$-0.30\,E_{\rm c.m.}$	−7.7	6.7	0.4	0.13

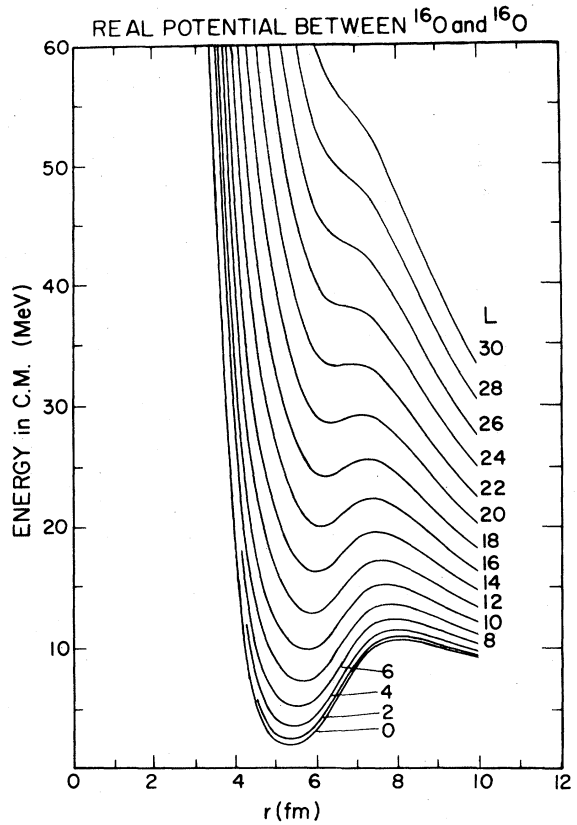

FIG. 3. Real potentials for the ^{16}O+^{16}O system. These potentials are composed of nuclear, Coulomb, and centrifugal parts. The nuclear part of the potential is chosen to be a two range Woods-Saxon shape given in Eq. (16). The Coulomb part is given by Eq. (5). Potential parameters corresponding to this figure are given in Table I.

parameter R of the attractive potential as follows:

$$R = R_0\left\{2 + \sum_\mu \frac{\gamma}{\sqrt{7}}\left[b_{3\mu} + (-)^\mu b^\dagger_{3-\mu}\right]Y_{3\mu}(\hat{r}) + \sum_\mu \frac{\gamma}{\sqrt{7}}\left[b_{3\mu} + (-)^\mu b^\dagger_{3-\mu}\right]Y_{3\mu}(-\hat{r})\right\}, \quad (18)$$

where R_0 and γ are the mean radius of the oxygen nucleus and the coupling parameter to the 3^-_1 excitation, respectively. In our calculation we retain only the first order term in the expansion of the attractive potential in powers of γ. As a result, we obtain the following coupling potential using Eq. (14):

$$V_{cc'}(r) = -\gamma\frac{RV}{2}\frac{d}{dr}\left[f_{\rm WS}(R,a,r)\right](2\pi)^{-1/2}\hat{L}_c\hat{L}_{c'} \times (L_cL_{c'}00\,|\,30)W(I_cL_cI_{c'}L_{c'};J3)(1-\delta_{I_cJ_{c'}}), \quad (19)$$

where $\hat{L}$ and $W(abcd;ef)$ represent the factor $(2L+1)^{1/2}$ and the Racah coefficient, respectively.

We have adjusted the coupling strength γ to reproduce the amplitude of the structure in the observed excitation function for the total gamma-radiation yield from the 3^-_1 state and the value thus chosen, $\gamma = 0.13$, is found to be consistent with that previously used in a study of the ^{12}C + ^{16}O system,[13,18] i.e., $\gamma = 0.1$.

For the imaginary part, the angular momentum dependent imaginary potential suggested by Chatwin *et al.*[38] has been incorporated directly in our model. It is given as follows:

$$\mathrm{Im}U_{\rm opt}(r) = W f_{\rm WS}(R,a,r) f_{\rm WS}(J_c, \Delta J, J), \quad (20)$$

where

$$J_c = \bar{R}[(2\mu/\hbar^2)(E+\bar{Q})]^{1/2}. \quad (21)$$

Adopted parameters are listed in Table I. They are close to those of Chatwin *et al.*[38] The same imaginary potentials have been assumed for both elastic and inelastic channels.

We emphasize that the angular momentum dependence of the imaginary potential—such that the grazing partial waves are only weakly absorbed—plays a very important role in the BCM in reproducing both the widths of characteristic energy dependent structure and the magnitude of the fusion cross section. This angular momentum dependence is physically reasonable as reflecting a low level density of high spin states in the vicinity of the yrast line.

C. Cross sections

We have calculated various cross sections using S-matrix elements which are obtained by solving the coupled-channel equation (12) and the above mentioned model parameters. Because of the

TABLE II. Predicted energies and single particle widths of resonances in the elastic and 3^-_1 inelastic channels. In this calculation, the coupling and imaginary potentials are switched off. The other potential parameters are those of Table I. Heights of potential barriers are also listed.

	Elastic channel			3^-_1 aligned channel		
J^π	$E^{(0)}_J$ (MeV)	Γ_{sp} (MeV)	$B^{(0)}_J$ (MeV)	$E^{(3)}_J$ (MeV)	Γ_{sp} (MeV)	$B^{(3)}_J$ (MeV)
14^+	19.0	0.42	19.6	20.4	0.06	22.3
16^+	22.6	0.95	22.4	23.5	0.24	24.5
18^+	26.6	1.8	25.6	26.9	0.65	27.1
20^+	31.0	2.8	29.3	30.7	1.3	30.1
22^+	35.8	3.9	33.5	35.1	2.3	33.5
24^+	41.0	4.7		39.5	3.4	37.4

symmetry in the entrance channel, expressions for cross sections for $^{16}O+^{16}O$ scattering necessarily differ from those for nonidentical particle collision. Here we summarize the expressions we have used.

The differential cross section for elastic scattering is given as follows:

$$\frac{d\sigma_{el}}{d\Omega} = \left| f_c(\theta) + f_c(\pi-\theta) + \left(\frac{i}{k}\right) \times \sum_{J:\text{even}} (2J+1) e^{2i\sigma_J} (1 - S^J_{cc}) P_J(\cos\theta) \right|^2 , \tag{22}$$

where $f_c(\theta)$, σ_J, S^J_{cc}, and $P_J(x)$ are the Coulomb scattering amplitude, the Coulomb phase shift, the elastic scattering S matrix, and the Legendre polynomial, respectively. The summation in Eq. (22) covers only even J values.

Angle integrated cross sections for inelastic scattering are given as follows:

$$\sigma_{inel} = \frac{2\pi}{k^2} \sum_{c'} \sum_{J:\text{even}} (2J+1) |S^J_{c'c}|^2 , \tag{23}$$

where $S^J_{c'c}$ is the inelastic scattering S matrix and c' represents inelastic channels. In our case only the 3^-_1 aligned channel is included.

The total reaction cross section is defined in terms of the flux removed from the elastic channel and is given as follows:

$$\sigma_R = \frac{2\pi}{k^2} \sum_{J:\text{even}} (2J+1)(1 - |S^J_{cc}|^2) . \tag{24}$$

Using these expressions, the total fusion cross section may reasonably be defined as the difference between the total reaction cross section and total cross section for inelastic scattering and is given simply as

$$\sigma_{fus} = \sigma_R - \sigma_{inel} . \tag{25}$$

IV. RESULTS AND DISCUSSION

In this section we present the results of our numerical calculations and compare them with experimental data.

A. 3^-_1 inelastic cross section

In Fig. 4 we compare our calculated 3^-_1 inelastic excitation function for $^{16}O+^{16}O$ scattering with the gamma-radiation yield data measured by Kolata *et al.*[4] The fact that the measured cross sections are systematically larger than those calculated may reflect other contributions to the yield of 3^-_1 gamma radiation in addition to that from the single 3^-_1 inelastic scattering process included in our calculation. Some of the difference may be attributed to contributions from the mutual 3^-_1 inelastic scattering which was not taken into account in the present calculations and whose aligned band crosses the elastic one at an energy slightly higher than that of the single 3^-_1 band as is shown in Fig. 2. Data are not yet available on this mutual excitation channel. Among other reactions, which will contribute with increasing intensity to the gamma-radiation yield as the bombarding energy is increased, are inelastic scattering to states in ^{16}O higher than 6.13 MeV in excitation—which thereafter deexcite via cascades through that state—as well as reactions leading to a $^{12}C+^{20}Ne$ final channel, wherein the excited ^{20}Ne subsequently decay to excited states in ^{16}O which deexcite either in cascade or directly from the 6.13 MeV 3^-_1 state. Because these noninelastic contributions to the 6.13 MeV gamma-radiation yield can include effects of many partial waves, they might be expected to increase smoothly as a function of energy, as does the apparent background underlying the structure in the data. A good example of such a background contribution may be found in the $^{12}C+^{12}C$ scattering in which gamma-radiation yields[39] deexciting the 4.44 MeV 2^+_1 state of ^{12}C show increasing background when compared with the pure 2^+_1 inelastic scattering data.[40] It bears noting that Refs. 7 and 10 regarded the 3^-_1 gamma-radiation yield data of the $^{16}O+^{16}O$ system as if they are pure 3^-_1 inelastic cross sections. In this respect, direct measurements on inelastic cross sections for the single and mutual 3^-_1 inelastic excitations in the $^{16}O+^{16}O$ system would be important.

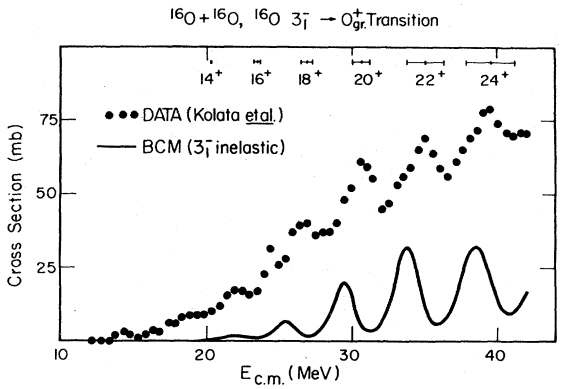

FIG. 4. Inelastic 3^-_1 cross sections in $^{16}O+^{16}O$ scattering. The solid line shows the angle integrated inelastic cross sections predicted by coupled-channel calculations based on the BCM. Data for gamma radiation deexciting the 3^-_1 state of ^{16}O measured by Kolata *et al.* (Ref. 4), are also indicated. Energies, widths, and total angular momenta of zeroth order resonances in the aligned 3^-_1 rotational band are shown in the upper part of the panel.

What appears gratifying, however, is that the energy intervals, widths, and amplitude of the struc-

ture that appears to be superimposed on a monotonically increasing background in the experimental data are reproduced reasonably well by the predicted curve. Each peak of the calculated cross section corresponds to each partial wave with subsequent total angular momentum. It is found that if we allow minor changes in the interaction potential for the inelastic channel, small shifts in the calculated peak positions can easily be obtained without significantly reducing the quality of the fits to the fusion and elastic data. However, we have preferred to adopt a simple assumption, i.e., the same interaction for both elastic and inelastic channels, and to demonstrate how close they come to reproduce the data without any modification rather than attempting to fine tune.

In the upper part of Fig. 4, energies, widths, and total angular momenta of the zeroth order states in the aligned rotational band are shown. It is obvious that the energies and widths of the calculated structure correspond reasonably to those of the original states. This supports the validity of the schematic discussion of the BCM given in Sec. II.

B. Elastic excitation functions

Elastic $^{16}O+^{16}O$ excitation functions were also calculated with this model. In Fig. 5 they are compared with data of Maher *et al.*[5] for all five measured angles; $\theta_{c.m.}=49.3°$, 60.0°, 69.8°, 80.3°, and 90.0°. Characteristic gross features of the data are well reproduced by our coupled-channel calculation at all angles. These excitation functions are one of the examples which have been studied by many different approaches. For example, Maher *et al.*,[5] Gobbi *et al.*,[23] Chatwin *et al.*,[38] and Baye *et al.*[24] have all reproduced these data quite well within different frameworks which take only the elastic channel into account explicitly. The quality of our reproduction of these data is comparable to that obtained by all of these groups. The advantage of the BCM is that this model can reproduce not only the elastic scattering but also other data, i.e., fusion and inelastic cross sections at the same time. It should be emphasized that Fig. 5 is plotted not on a semilogarithmic scale but on a linear one and thus tends to emphasize discrepancies.

We have also calculated these excitation functions without the coupling potential, i.e., as a simple optical model calculation with our parameters. Characteristic features of the results are quite similar to those of Fig. 5. In this respect the gross oscillatory structure of the elastic $^{16}O+^{16}O$ excitation functions can be understood as entrance channel phenomena.

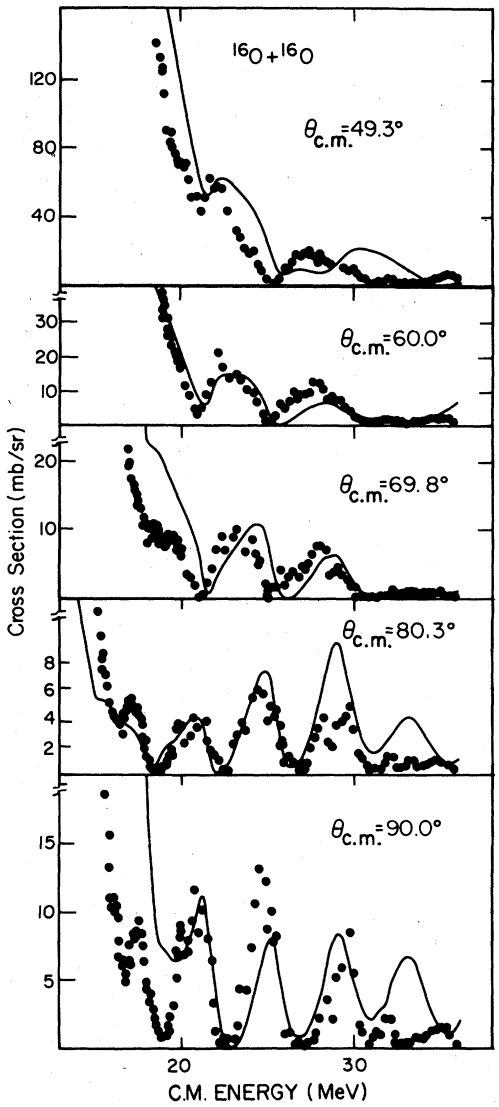

FIG. 5. Elastic scattering excitation functions for the $^{16}O+^{16}O$ system. Calculated elastic scattering excitation functions are compared with data of Maher *et al.* (Ref. 5) for five measured angles, i.e., $\theta_{c.m.}=49.3°$, 60.0°, 69.8°, 80.3°, and 90.0°. Characteristic gross features of the data are well reproduced by our coupled-channel calculations for all angles. This figure is plotted on a linear scale.

Our calculations do not predict the fragmentation of the gross maxima in the elastic scattering excitation function obtained by Scheid *et al.*,[6] and apparent in the experimental data.[5] This may reflect our use of the same imaginary potential in both elastic and inelastic channels whereas Scheid *et al.*[6] used a substantially weaker imaginary potential in the inelastic channel. The widths of the observed intermediate structure in the elastic excitation function is typically ~300 keV,[5] while the

characteristic width of the observed structure of the gamma-radiation data which can be reproduced by our model is 1–3 MeV. This may suggest different origins for these structure. It would be very interesting to learn whether the gamma-radiation yield data show structure of few hundred keV width or not; currently available data are not adequate to answer this question.

C. Fusion cross section

In the middle panel of Fig. 6 we compare our model prediction with experimental fusion data of Fernandez *et al.*[3] Obviously the magnitude and oscillatory structure of the data are well reproduced. In the center of Fig. 6 we also show the calculated contribution to the total fusion cross section from each individual partial wave. The oscillatory structure in the fusion excitation function can be identified readily with the contribution from each new partial wave as it becomes active with increasing energy. In the top panel of Fig. 6 we show the behavior of the optical model phase shift (calculated with W set equal to zero for clarity). The resonance energy of each grazing partial wave, where the real phase shift passes through 90° and has a positive slope, corresponds to the peak of each partial fusion cross section. As noted in our preliminary reports,[19] this fact may suggest that each oscillation of the fusion data reflects the existence of shape resonances of grazing partial waves in the entrance channel.

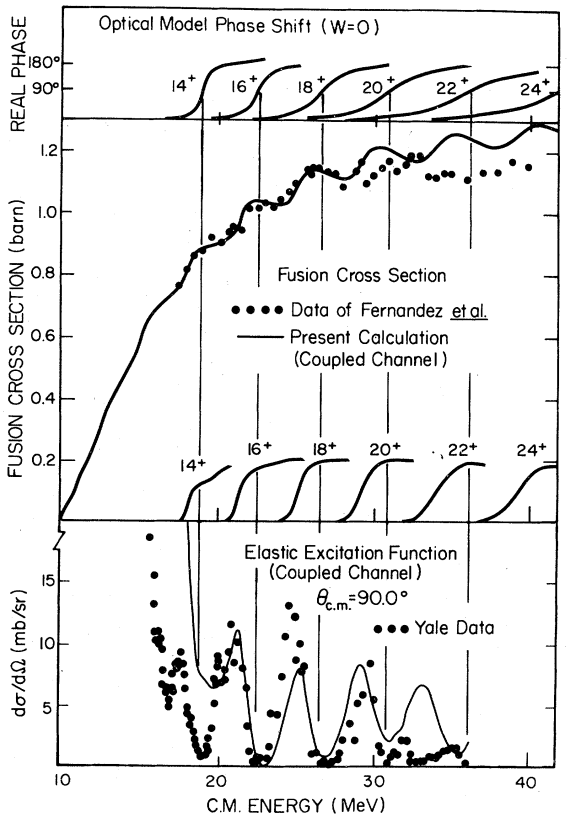

FIG. 6. Fusion cross sections for the $^{16}O+^{16}O$ system. In the middle panel, calculated total fusion cross sections are compared with experimental data of Fernandez *et al.* (Ref. 3). The calculated contribution to the total fusion cross section from each identified partial wave is also shown in the center of the figure. In the upper panel, real phase shifts for the elastic $^{16}O+^{16}O$ scattering (without absorption) are shown. In the lower panel, the 90° elastic scattering excitation function of Fig. 5 is reproduced.

Other possible origins for structure in the fusion excitation function include barrier penetration effects and a possible energy dependence of the imaginary potential depth. To study these effects of barrier penetration on the fusion cross section, we have also calculated total reaction cross sections using a semiclassical model[41] that is intrinsically free from resonances. In this model the potential shape in the region of the outer barrier is approximated by an inverted parabolic form, and strong absorption is assumed inside of the potential barrier. Then the total reaction cross section, Eq. (24), can be expressed as follows[41]:

$$\sigma_R = \frac{2\pi}{k^2} \sum_{J:\text{even}} (2J+1) T_J \,, \tag{26}$$

where the transmission coefficient T_J is

$$T_J = \{1 + \exp[2\pi(B_J^{(0)} - E)/\hbar\omega_J]\}^{-1} \,, \tag{27}$$

$$\hbar\omega_J = \hbar \left\{ \frac{1}{\mu} \left| \frac{d^2}{dr^2} \left[\frac{\hbar^2 J(J+1)}{2\mu r^2} + \mathrm{Re}U_{\mathrm{opt}}(r) \right] \right|_{r=R_b} \right\}^{1/2} . \tag{28}$$

$B_J^{(0)}$ is the barrier height discussed in Sec. II and given in Table II. $\hbar\omega_J$ and $\mathrm{Re}U_{\mathrm{opt}}(r)$ are the harmonic oscillator constants of the inverted parabolic form and the real part of the optical potential adopted in our coupled-channel calculations, respectively. In Fig. 7 calculated total reaction cross sections are shown by the solid line. Fusion data of Fernandez *et al.*[3] and of Kolata *et al.*,[21] which were obtained using different experimental methods, are also shown. The result shows no oscillatory structure, except in the higher energy region where the assumed inverted parabolic form fails to fit the outer potential barrier for the corresponding partial waves (see Fig. 3). On the other hand, the total reaction cross sections predicted by the BCM—which can be given by Eq. (25), i.e., a summation of the total fusion cross section σ_{fus} and the total inelastic cross section σ_{inel}—do show oscillatory structure. Comparison between the

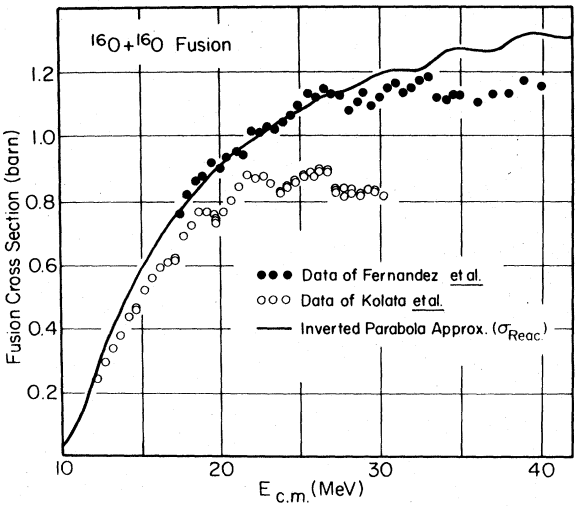

FIG. 7. Total reaction cross sections in the $^{16}O+^{16}O$ system. The solid line shows the total reaction cross section estimated by a strong absorption model described in the text. Data (Refs. 3, 21) on total fusion cross sections measured using two different experimental methods are also shown.

two calculational results may illuminate the effects of resonances, the existence of which enhances the absorption at resonance energies. In other words, the steep increase of the partial fusion cross section of Fig. 6 cannot be ascribed to the effects of barrier penetration.

Although Phillips *et al.*[7] obtain a reasonable reproduction of some of the data without explicit use of resonances, the steep energy dependence of their parametrized transmission coefficients is not produced by the strong absorption model described above, and it may be a concealed effect of underlying resonances. This should not be surprising, because their S matrix simulates that of Gobbi,[23] in which resonances play an important role. It should be noted that the parabolic potential barrier adopted in this barrier penetration calculation is not arbitrary, but is a physically reasonable one, since this barrier simulates our potential, which can reproduce elastic scattering correctly.

The effects of energy dependence of the imaginary potential, which is introduced into our calculation through the energy dependence of the critical angular momentum J_c, have also been studied. Calculations of total reaction cross sections using an optical model with the same imaginary potential and changing energies of resonances suggest that the existence of resonances plays a crucial role in the reproduction of the fusion structure at energies of ~19, ~22, and ~26 MeV where both the Fernandez[3] and Kolata[21] data sets show prominent fusion oscillation. However, calculated fusion structure of Fig. 6 at higher energies, i.e., ~30, ~35, and ~40 MeV, reflects mainly the effects of the energy dependence of our imaginary potential. This energy- and angular momentum dependence of absorption effects are interesting topics in the study of heavy ion interactions and we are extending our studies of them.

Kolata *et al.*[21] have already noted an anticorrelation between the structure in the fusion data and that in the 90° elastic scattering excitation function for the $^{16}O+^{16}O$ system. As shown in the lower panel of Fig. 6, the minima in the 90° excitation function correspond to the resonances in the entrance channel and reflect destructive interference between the resonance and background elastic amplitudes. This clearly explains the anticorrelation between the structure in the fusion data and that in the 90° elastic scattering excitation function.

In the past, the gross maxima in the 90° elastic scattering excitation function for $^{16}O+^{16}O$ scattering have frequently been taken to present the resonances. Baye *et al.*,[24] for example, reported that this interpretation had been demonstrated explicitly by their satisfactory reproduction of the elastic excitation functions.

This apparent discrepancy in the identification of resonance energies from the elastic scattering data may be resolved readily. In addition to the real phase shifts δ_J—which are calculated explicitly by the microscopic R-matrix theory—Baye *et al.*[24] introduced smooth cutoff coefficients $A_J(E)$ into the S matrix to take absorption effects into account:

$$S^J_{cc}=A_J(E)e^{2i\delta_J}, \tag{29}$$

where

$$A_J(E)=f_{WS}(\bar{E}_J,\Delta E,E). \tag{30}$$

ΔE is a diffuseness parameter and taken to be 1 MeV for all J values. $\bar{E}_J$ is the energy where $|S^J_{cc}|=0.5$. In their data reproduction, the parameters $\bar{E}_J$'s were set of 19.3, 22.8, 26.8, 31.2, 36.1, and 41.5 MeV for $J=14$, 16, 18, 20, 22, and 24, respectively. These values are very close to our resonance energies for the elastic band as listed in Table II, which play a dominant role in our reproduction of the elastic excitation functions.

We have searched for possible influence of inelastic channels other than the aligned one, by comparing the results presented herein with those obtained using a full coupled-channel calculation including all four inelastic 3^-_1 channels. There appears to be no meaningful difference for any of the calculated cross sections that we reported here, which supports the validity of our truncation of the model space suggested by the BCM.

V. SUMMARY AND CONCLUSION

We have shown that a schematic discussion of a band-crossing model can explain the existence of a sequence of resonance-like peaks observed in the yield of 6.13 MeV gamma radiation as a consequence of strong mixing of wave functions in the elastic and 3_1^- aligned inelastic bands, respectively, in the energy region where these bands approach and cross. A simple coupled-channel calculation based on the BCM, in which only the elastic and the 3_1^- aligned inelastic channels are included, provides a quite reasonable reproduction of all currently available data on the energy dependence of cross sections in the $^{16}O+^{16}O$ interactions, i.e., the 3_1^- gamma radiation yield,[3] total fusion,[4] and elastic scattering[5] data. The structure in the fusion excitation function and the gross structure in the elastic scattering excitation functions can be understood as entrance channel phenomena, which reflect shape resonances for individual grazing partial waves in the entrance channel. The resonance energies in the entrance channel were shown to correspond not to maxima but to minima in the 90° elastic scattering excitation function. In this way the observed anticorrelation between fusion and 90° elastic scattering excitation function was explained naturally. Our results for the 3_1^- inelastic cross section provide additional support for the physical validity of the BCM discussed in Sec. II.

An angular momentum dependent imaginary potential in which the grazing partial wave feels weak absorption and lower angular momentum partial waves feel strong absorption plays an important role in our reproduction of both the widths of structure in the gamma-radiation yield and the magnitude of the fusion cross section. This is a common feature for all the $^{12}C+^{12}C$, $^{12}C+^{16}O$, and $^{16}O+^{16}O$ systems which have been studied using the BCM. In this respect simple strong absorption models may not be a good assumption for these systems.

From these results we are led to conclude that our examination of all the available data suggests that nuclear molecular resonances are indeed responsible for the energy dependent structure in the $^{16}O+^{16}O$ system as well as in the $^{12}C+^{12}C$ system. The lack of comparable resonant structure in the total reaction cross sections in the Coulomb barrier region in the $^{16}O+^{16}O$ system reflects not the absence of nuclear molecular phenomena but rather their being masked by a great many competing nonresonant amplitudes as originally noted by Hanson *et al.*[42]

ACKNOWLEDGMENTS

The authors thank Dr. T. Matsuse and members of the A. W. Wright Nuclear Structure Laboratory for helpful discussion. We are grateful to Dr. F. Haas for providing us with his data prior to publication. They wish to thank Professor N. Austern for his careful reading of the manuscript and for his suggestions concerning it. This work was supported by the U. S. Department of Energy under Contract No. EY-76-C-02-3074.

---

*Present address: Nuclear Physics Laboratory, University of Pittsburgh, Pittsburgh, Pa. 15260.

[1]E. Almqvist, D. A. Bromley, and J. A. Kuehner, Phys. Rev. Lett. 4, 515 (1960).

[2]For example, D. A. Bromley, *Nuclear Molecular Phenomena*, edited by N. Cindro (North-Holland, Amsterdam, 1978), p. 3.

[3]B. Fernandez, C. Gaarde, J. S. Larsen, S. Pontoppidan, and F. Videbaek, Nucl. Phys. A306, 259 (1978).

[4]J. J. Kolata, R. M. Freeman, F. Haas, B. Heusch, and A. Gallmann, Phys. Rev. C 19, 2237 (1979).

[5]J. V. Maher, M. W. Sachs, R. H. Siemssen, A. Weidinger, and D. A. Bromley, Phys. Rev. 188, 1665 (1969).

[6]W. Scheid, W. Greiner, and R. Lemmer, Phys. Rev. Lett. 25, 176 (1970).

[7]R. L. Phillips, K. A. Erb, D. A. Bromley, and J. Weneser, Phys. Rev. Lett. 42, 566 (1979).

[8]F. J. W. Hahne, Nucl. Phys. A104, 545 (1967).

[9]N. Austern and J. S. Blair, Ann. Phys. (N.Y.) 33, 15 (1965).

[10]W. A. Friedman, K. W. McVoy, and M. C. Nemes, Phys. Lett. 87B, 179 (1979).

[11]O. Tanimura, Nucl. Phys. A309, 233 (1978).

[12]Y. Kondō, T. Matsuse, and Y. Abe, in *Proceedings of the INS-IPCR Symposium on Cluster Structure of Nuclei and Transfer Reactions Induced by Heavy-Ions, Tokyo*, edited by H. Kamitsubo, I. Kohno, and T. Marumori (The Institute of Physical and Chemical Research, Wako-Shi, Saitama, Japan, 1975), p. 280; Y. Abe, *Proceedings of the Second International Conference on Clustering Phenomena in Nuclei, College Park, Maryland, 1975*, edited by D. Goldman, J. B. Marion, and S. J. Wallace (National Technical Information Service, Springfield, Virginia, 1975), p. 500.

[13]T. Matsuse, Y. Kondō, and Y. Abe, Prog. Theor. Phys. 59, 1009 (1978).

[14]Y. Abe, Y. Kondō, and T. Matsuse, Prog. Theor. Phys. 59, 1393 (1978).

[15]Y. Kondō, Y. Abe, and T. Matsuse, Phys. Rev. C 19, 1356 (1979).

[16]Y. Abe, T. Matsuse, and Y. Kondō, Phys. Rev. C 19, 1365 (1979).

[17]T. Matsuse, Y. Abe, and Y. Kondō, Prog. Theor. Phys. 59, 1037 (1978).

[18]T. Matsuse, Y. Abe, and Y. Kondō, Prog. Theor. Phys. 59, 1904 (1978).

[19]Y. Kondō and D. A. Bromley, Bull. Am. Phys. Soc. 24,

556 (1979); Y. Kondō, D. A. Bromley, and Y. Abe, Prog. Theor. Phys. 63, 722 (1980).
[20]Y. Abe, Y. Kondō, and T. Matsuse, Suppl. of Prog. Theor. Phys. (to be published).
[21]J. J. Kolata, R. C. Fuller, R. M. Freeman, F. Haas, B. Heusch, and A. Gallmann, Phys. Rev. C 16, 891 (1977).
[22]A. Arima, G. Scharff-Goldhaber, and K. W. McVoy, Phys. Lett. 40B, 7 (1972).
[23]A. Gobbi, R. Wieland, L. Chua, and D. A. Bromley, Phys. Rev. C 7, 30 (1973).
[24]D. Baye and P.-H. Heenen, Nucl. Phys. A276, 354 (1977).
[25]L. F. Canto, Nucl. Phys. A279, 97 (1977).
[26]T. Ando, K. Ikeda, and A. Tohsaki-Suzuki, Prog. Theor. Phys. 61, 101 (1979) and references therein.
[27]P. P. Singh, D. A. Sink, P. Schwandt, R. E. Malmin, and R. H. Siemssen, Phys. Rev. Lett. 28, 1714 (1972).
[28]M. Nogami, private communication.
[29]B. Imanishi, Nucl. Phys. A125, 33 (1969).
[30]Y. Suzuki, Prog. Theor. Phys. 55, 1751 (1976); 56, 111 (1976).
[31]B. R. Fulton, T. M. Cormier, and B. J. Herman, Phys. Rev. C 21, 198 (1980).
[32]Y. Mito and M. Kamimura, Prog. Theor. Phys. 56, 583 (1976).
[33]W. Kohn, Phys. Rev. 74, 1763 (1948).
[34]I. Shimodaya, R. Tamagaki, and H. Tanaka, Prog. Theor. Phys. 27, 793 (1962).
[35]R. Tamagaki and H. Tanaka, Prog. Theor. Phys. 34, 191 (1965).
[36]S. Okai and S. C. Park, Phys. Rev. 145, 787 (1966).
[37]T. Tamura, Rev. Mod. Phys. 37, 679 (1965).
[38]R. A. Chatwin, J. S. Eck, D. Robson, and A. Richter, Phys. Rev. C 1, 795 (1970).
[39]T. M. Cormier, J. Applegate, G. M. Berkowitz, P. Braun-Munzinger, P. M. Cormier, J. W. Harris, C. M. Jachcinski, L. L. Lee, Jr., J. Barrette, and H. E. Wegner, Phys. Rev. Lett. 38, 940 (1977).
[40]T. M. Cormier, C. M. Jachcinski, G. M. Berkowitz, P. Braun-Munzinger, P. M. Cormier, M. Gai, J. W. Harris, J. Barrette, and H. E. Wegner, Phys. Rev. Lett. 40, 924 (1978).
[41]K. W. Ford, D. L. Hill, M. Wakano, and J. A. Wheeler, Ann. Phys. (N.Y.) 7, 239 (1959).
[42]D. L. Hanson, R. G. Stokstad, K. A. Erb, C. Olmer, M. W. Sachs, and D. A. Bromley, Phys. Rev. C 9, 1760 (1974).